

Article ID: 1003 - 6326(2005)04 - 0889 - 08

Effect of n -Al₂O₃ on electrochemical nucleation and chemical binding interaction in nickel electrodeposition^①

TU Weiyi(涂伟毅), XU Binshi(涂滨士),

DONG Shirun(董世运), JIANG Bin(蒋斌), DU Lingzhong(杜令忠)

(State Key Laboratory of Remanufacture Technology, Armored Force Engineering Institute, Beijing 100072, China)

Abstract: The electrochemical nucleation mechanism of nickel on the vitreous carbon electrode from n -Al₂O₃/Ni composite brush plating system was investigated using potential step method. The interaction between nano- α -alumina and matrix metal was researched by X-ray photoelectron spectrometry. The results show that the nano- α -alumina leads to the increasing of the nuclei density, nucleation rate constant and crystal growth rate during nickel electrocrystallization. Nano- α -alumina is found to be beneficial for nucleation and growth of nickel. During the electrodeposition process, some nanoparticles are captured effectively on the growing metal surface. As the absorbed nickel atoms are diffusing on electrode surface, some of them arrive at the interface between the captured nano- α -alumina and the growing metal surface. The unsaturated bond of oxygen on nano- α -alumina surface can capture some of the absorbed nickel atoms and form nickel-oxygen chemical bond. The new nucleation and growth sites of nickel atoms appear at the interfaces between nanoparticles and metal growing surface. Nanoparticles are embedded gradually in the newly deposited nickel atoms, which leads to the formation of the composite coating. The results indicate that the nano- α -alumina takes part in the electrode reaction and the unsaturated chemical bond of oxygen on nanoparticle surface can combine with the absorbed nickel atoms by way of chemical bond.

Key words: nanoparticle; composite electrodeposition; chemical bond; co-deposition mechanism

CLC number: TG 174.441; TB 383

Document code: A

1 INTRODUCTION

In recent years, nanometer composite electric brush plating technology has been developed. It is a kind of novel surface repairing technology, which can prepare excellent surface coating^[1-7]. The technology is at the stage of development, its foundational theory and application field must be expanded. Up to now, investigations have been mainly focused on preparing coating, testing performance and developing new brush-plating solution, little attention is paid to the study on electrochemistry properties during the electrodeposition process and interaction between nanoparticles and matrix metal in composite coating. Although the fundamental research on surface characteristics of nanoparticles in solution and microstructure in composite coating has been done to reveal nanometer brush-plating process^[3, 8-10], the study on electrochemistry fundament and chemical combination state of nanoparticles in composite coating has not been reported in the case of composite electrobrush plating.

Electrochemical nucleation is an important growth mode of nickel electrocrystallization. The effect of nanoparticles on electrodeposition mechanism is a key factor determining the structure and performance of composite coating. In this paper, potential step was used for determining the electrochemical transient response from n -Al₂O₃/Ni composite brush plating solution and quick nickel solution. The electrochemical nucleation mechanism was studied and compared with each other. The effect of nanoparticles was discussed. The X-ray photoelectron spectrometry (XPS) of pure nickel and composite coating was measured. The results show that the nanoparticles take part in electrocrystallization, reduce the electrodeposition overpotential, enhance the current efficiency, and accelerate nucleation rate as well as crystal growth rate. Nanoparticles combine with nickel atoms in the composite coating by means of chemical bond and they are not mixed together mechanically. Nanoparticles not only influence the electrochemical mechanism during the composite electrodeposition, but also change the microstructure of

① **Foundation item:** Project(50235030) supported by the National Natural Science Foundation of China; Project(G1999065009) supported by the National Key Fundamental Project of China; Project(2002M3) supported by the Cooperative Foundation of Science and Technology of Sino-Britain Government

Received date: 2004-09-16; **Accepted date:** 2005-04-27

Correspondence: TU Weiyi, Associate Professor, PhD; Tel: + 86-996-2358783; E-mail: weiyitu@sohu.com

composite coating in some way.

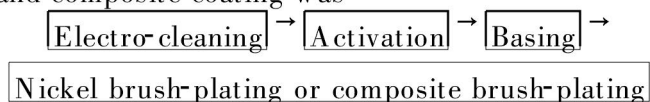
2 EXPERIMENTAL

2.1 Electrochemical experiment

The experimental cell was designed as a three-electrode system. The vitreous carbon electrode was employed for the working electrode with diameter of 2 mm. A platinum sheet with size of 8 mm × 15 mm was used as the counter electrode, and a saturation calomel electrode (SCE) was selected as the reference electrode. All potentials were measured and quoted with relative to SCE. The surface of the vitreous carbon electrode was polished to a mirror finish using metallurgical coated abrasive paper and alumina powder down to 0.3 μm in turn before each experiment. Then, the electrode was ultrasonicated and thoroughly rinsed with distilled water, acetone, distilled water successively, and at last transferred to the brush-plating solution with a layer of liquid membrane on electrode surface.

All electrochemical experiments were performed in quick nickel plating solution or composite solution. The solution contained 264 g/L NiSO₄ · 6H₂O, 56 g/L ammonium citrate, 23 g/L ammonium acetate, 105 g/L ammonia water and 20 g/L *m*-Al₂O₃. The original diameter of nanoparticles was in the range of 30–50 nm for nano-Al₂O₃. The pH of plating solution was adjusted to the desired range from 7.0 to 7.4. All the solution was prepared from analytical grade reagents and distilled water. The solution was bubbled with N₂ for 10 min before each experiment in order to eliminate the dissolved oxygen. The working electrode was held at potential 0 mV for 2 min before each measurement to ensure reproducible initial steady state on its surface. All experiments were carried out at the temperature of (20 ± 2) °C.

All electrochemical measurements were performed with Potentiostat/Galvanostat Model 273A (EG&G Instrumental Inc.). The computer controlled electrochemical system was used in recording the transient response. All coatings were prepared by means of electric brush-plating technology and DSD-75-S direct current power was used (Armored Force Engineering Institute). The technology procedure for preparing quick nickel and composite coating was



The coating thickness was about 100 μm. The diameter of nanoparticles distributes in the range of 30–50 nm and its mass content was about 1% in composite coating^[8, 10].

2.2 Spectrum experiment

The coating with the proper size was used for XPS testing. XPS measurement was performed using ESCA LAB220F-XL (VG Scientific). The position sensitive detector (PSD) and aluminium anode target were used with photon energy 1486.6 eV. The pressure in the vacuum room was kept at 2.9×10^{-7} Pa. C 1s with energy of 284.6 eV was used to calibrate spectral series displacement. Before testing the surface of solid samples was sputtered by argon ion, with sputtering rate of 4 nm/min, and lasting for 2 min. The emissive current was 25 mA and potential 3.0 kV. The powder sample was not sputtered.

3 RESULTS AND DISCUSSION

3.1 Effect of nanoparticles on potential step transient

The current–time curves of nickel on vitreous carbon electrode are shown in Figs. 1 and 2 in the potential range of –0.98–1.35 V.

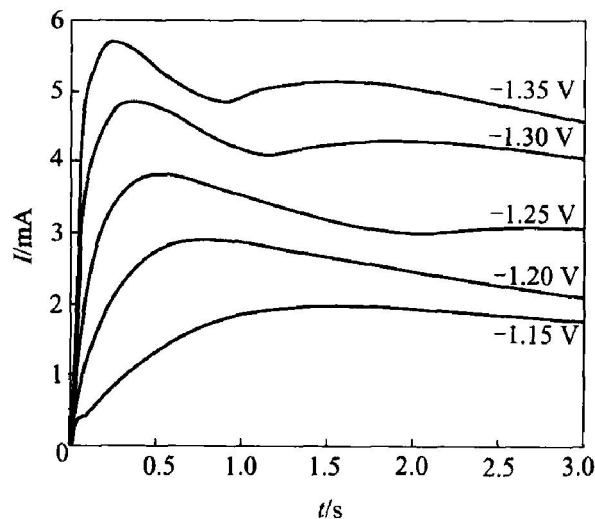


Fig. 1 Current–time curves obtained in quickly nickel brush plating solution (Number in plots is step potential)

Figs. 1 and 2 show the general feature of the current–time curves, which is commonly observed during the initial stages of the electrocrystallization of nickel on vitreous carbon substrates^[11–14]. When a step potential is employed, the current rises after the induction time and then arrives at the maximum value, finally approaches the steady state slowly. The higher the step potentials are, the more rapidly current drops. The peak current I_m becomes higher, while the peak time t_m becomes shorter as the step potential increases. It can be seen from the current–time curves at $\phi = -1.30$ V and $\phi = -1.35$ V that there is a current peak after maximum, which results from multi-nucleus

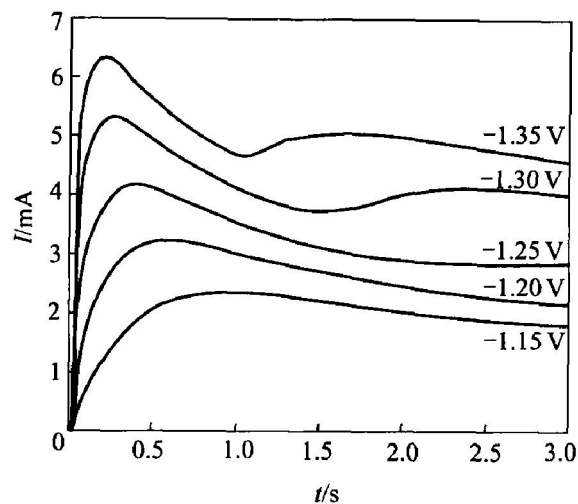


Fig. 2 Current-time curves obtained in γ -Al₂O₃/Ni composite brush plating solution (Number in plots is step potential)

growth and overlap^[13].

The current-time response in Fig. 2 shows the effect of nano-alumina on the nickel electrodeposition. Under the same experiment conditions, the current peaks in Fig. 2 are higher than those in Fig. 1, while the peak time in Fig. 2 is shorter. These facts show that nano-particles are favorable for nickel nucleation and crystal growth, nano-alumina takes part in nickel electrocrystallization.

3.2 Effect of nanoparticles on mechanism of nickel nucleation

According to the transient experimental results, some of electrocrystallization models were tried to verify the experimental data. It was found that these data were consistent with Scharifker hemisphere-multinucleus model better^[11-15]. On the basis of hemisphere model taking into account the overlap of three-dimensional multinucleus growth centers under the condition of diffusion control, Scharifker and his coworker derived the potentiostatic current-time equation^[15]. The relation between dimensionless parameters $(I/I_m)^2$ and t/t_m for progressive nucleation and instantaneous nucleation was different at the initial stages of electrodeposition, which provided a theoretical criterion for distinguishing between two nucleation kinetics^[15].

Figs. 3 and 4 show the relation between $(I/I_m)^2$ and t/t_m , derived from Figs. 1 and 2, respectively.

It can be seen from Figs. 3 and 4 that, these experimental data are consistent with the theoretical curves in potential ranges of -0.98 – 1.10 V and -0.98 – 1.07 V, respectively, which shows that the nickel electrocrystallization follows the mechanism of three-dimensional progressive nucleation. The experimental data are deflected from

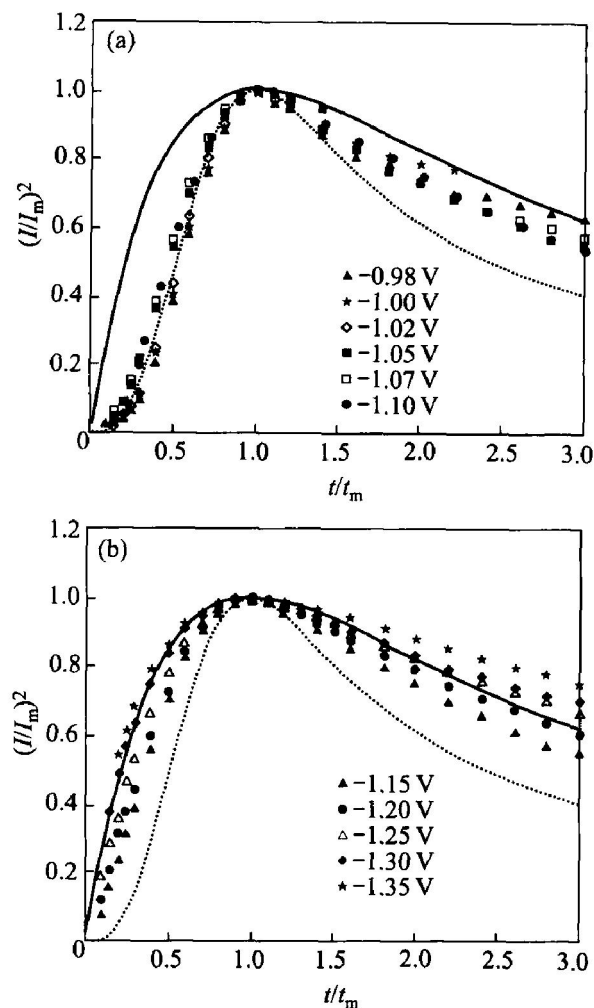


Fig. 3 Curves of $(I/I_m)^2$ vs t/t_m obtained in quickly nickel brush plating solution for instantaneous nucleation(a) and progressive nucleation(b) (Solid lines are theoretical curves, number in plots is step potential)

progressive nucleation theoretical curves and shifts to instantaneous nucleation theoretical ones with potentials in the range of -1.15 – 1.25 V and -1.10 – 1.20 V. When potentials are more negative than -1.30 V and -1.25 V, respectively, the experimental data are consistent with instantaneous nucleation theoretical curves, which shows that the nickel electrocrystallization is conformed to the mechanism of three-dimensional instantaneous nucleation.

The above results show that the dimensionless parameters $(I/I_m)^2$ rises with the increasing of step potentials and they are independent of γ -alumina, the electrocrystallization mechanism is changed from progressive nucleation to instantaneous nucleation gradually. Those results indicate that the enhanced cathode polarization can supply more growth centers, raises the nucleation rate and changes the electrocrystallization mechanism. Nanoparticles would accelerate the transformation of the progressive nucleation mechanism to instan-

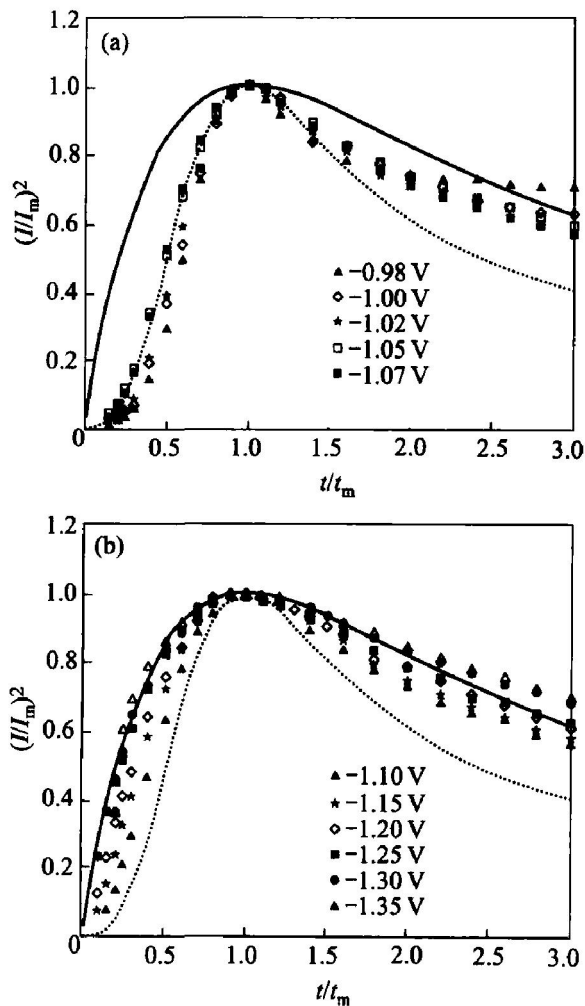


Fig. 4 Curves of $(I/I_m)^2$ vs t/t_m obtained in $n\text{-Al}_2\text{O}_3/\text{Ni}$ composite brush plating solution for instantaneous nucleation(a) and progressive nucleation(b) (Solid lines are theoretical curves, numbers in plots is step potential)

taneous nucleation one and promote the conversion of the active sites into growth centers on electrode surface. Nano-alumina takes part in electrode reaction but does not change the electrocrystallization mechanism of nickel.

3.3 Effect of nano-particles on electrocrystallization parameters of nickel

On the basis of nucleation theory, the electrocrystallization parameters of nickel can be calculated for progressive and instantaneous nucleation mechanism. Relative equations are as follows^[15]:

Progressive nucleation mechanism,

$$t_m = \left[\frac{4.6733}{A \pi k' D} \right]^{1/2} \quad (1)$$

$$I_m = 0.461 5nFD^{3/4} C(k'A)^{1/4} \quad (2)$$

$$I_m^2 t_m = 0.259 8(nFC)^2 D \quad (3)$$

$$N_{\text{sat}} = \left[\frac{A}{2k'D} \right]^{1/2} \quad (4)$$

$$k' = \frac{4}{3} \left[\frac{8\pi cM}{\rho} \right]^{1/2} \quad (5)$$

Instantaneous nucleation mechanism,

$$t_m = \frac{1.2564}{N_0 \pi k D} \quad (6)$$

$$I_m = 0.638 2nFD(kN_0)^{1/2} \quad (7)$$

$$I_m^2 t_m = 0.162 9(nFc)^2 D \quad (8)$$

$$k = \left[\frac{8\pi cM}{\rho} \right]^{1/2} \quad (9)$$

where I_m and t_m are the maximum current and the corresponding time in the transient curves. nF (C/mol) is the molecular charge. D (cm^2/s) and c (mol/L) are diffusion coefficient and concentration of nickel ion in solution respectively, A ($\text{nuclei} \cdot \text{cm}^{-2} \cdot \text{s}^{-1}$) is the nucleation rate constant, N_0 ($\text{nuclei}/\text{cm}^2$) is nuclei density for instantaneous nucleation and N_{sat} ($\text{nuclei}/\text{cm}^2$) is saturated nuclei density for progressive nucleation, M (g/mol) and ρ (g/cm^3) are relative molar mass and density of nickel deposit, respectively.

The growth rate constant in the direction perpendicular to the substrate K' ($\text{mol} \cdot \text{cm}^{-2} \cdot \text{s}^{-1}$) is given by^[16]

$$I_m = nFK' \quad (10)$$

The nuclei density and the nucleation rate constant can be calculated by Eqns. (1)-(5) and (6)-(10), respectively. Nucleation parameters of nickel electrocrystallization are listed in Table 1.

These data show that the nucleation parameters of nickel electrocrystallization depends on potential and nano-alumina. When nano-alumina are employed, all parameters are higher in composite solution than those in the quick nickel solution under the same experimental condition, which indicates further that nano-alumina takes part in electrocrystallization of nickel, promoting the nucleation and accelerating the growth of crystal.

According to the electrochemical nucleation theory, the rate at which adatoms are converted into nuclei is proportional to the probability that the adatoms exceed a certain energy level. The relation between the nucleation rate constant (A) and the critical nucleation growth activation energy is given by^[17]

$$A = k \exp \left[- \frac{\Delta G}{RT} \right] = k \exp \left[- \frac{k_1}{\eta^2} \right] \quad (11)$$

where k and k_1 are constant, ΔG is the critical nucleation growth activation energy and η is the overpotential of electrode reaction.

The nucleation rate constant (A) rises with the increasing value of η or decreasing with ΔG , and so are N_0 and N_{sat} , which leads to the decreasing of the size of crystal. These results are found to be consistent with experimental facts^[8, 10]. Under the same experimental condition, A is higher for the composite system than that for quick nickel system while ΔG is lower. Obviously, nano-particles would lower the activation energy of electrocrystallization, which proves that nano-particles

takes part in the electrode reaction, not in the physical way but in the chemical one.

The process of nickel electrodeposition is always accompanied by hydrogen evolution reaction (HER). The relation between current and potential is not linear in HER and the effect of HER on nickel electrodeposition is difficult to eliminate. So the kinetic data of nickel electrodeposition can not be analyzed quantitatively. But it is significant to compare and analyze parameters of electrocrystallization in the composite system and quick nickel one under the same experimental condition.

3.4 Combination state between nano-alumina and matrix nickel

In order to understand whether nano-alumina and matrix nickel are combined in the composite coating chemically or mechanically, X-ray photoelectron spectrometry is used for analyzing the energy state of elements in coating^[9].

The spectrograms of nickel element are depicted in Fig. 5 and the relative parameters are shown in Table 2.

From Figs. 5(a) and 5(b), it can be seen that peaks of nickel appear at the same binding energy but the proportion of areas for $\text{Ni}^{0} 2p_{3/2}$ peak and $\text{Ni}_2\text{O}_3 2p_{3/2}$ one for the pure nickel coating and composite one is different. According to the exper-

imental results in Fig. 5 and data in Table 2, it can be concluded that the two kinds of coating are composed of the same components with different relative contents^[18, 19].

If there were no chemical bond between matrix nickel and oxygen on nanoparticles, the proportion of nickel oxide to Ni^0 in composite coating would be close to that in quick nickel coating. In fact, relative content of nickel oxide in the composite coating is much higher than that in quick nickel coating. The reason is that the unsaturated chemical bond of oxygen from nanoparticles surface can combine with nickel atom from matrix metal and form $\text{Ni}-\text{O}$ chemical bond. The nickel oxides in the composite coating consisted of surface oxide and interior oxide, later mainly derives from $\text{Ni}-\text{O}$ chemical bond between matrix nickel and nanoparticles.

In the interior of coating, there was little nickel oxide derived from oxidized growth surface of matrix metal during plating process. Because the experimental conditions were the same for the preparing process of pure nickel and composite coating, the relative content of oxide should be close to each other in two kinds of coating. So the oxide from the preparing process is not the key factor for bringing about the different proportion of peak area between nickel oxide and Ni^0 in Fig. 5.

Table 1 Nucleation parameters of nickel electrocrystallization

Potential /V	N_0 or N_{sat} / (nuclei $\cdot \text{cm}^{-2}$)		K' / (mol $\cdot \text{cm}^{-2} \cdot \text{s}^{-1}$)		A / (cm $^{-2} \cdot \text{s}^{-1}$)	
	Ni	$n\text{-Al}_2\text{O}_3/\text{Ni}$	Ni	$n\text{-Al}_2\text{O}_3/\text{Ni}$	Ni	$n\text{-Al}_2\text{O}_3/\text{Ni}$
- 0.98	304 108.3	318 449.3	4.31×10^{-8}	4.75×10^{-8}	19 361	22 892
- 1.00	404 405.4	481 715.5	5.61×10^{-8}	6.48×10^{-8}	38 676	58 119
- 1.02	574 747.4	678 625	8.66×10^{-8}	9.67×10^{-8}	101 184	144 904
- 1.05	678 198.1	1 280 012	1.24×10^{-7}	1.39×10^{-7}	186 023	541 272
- 1.07	1 137 933	1 406 436	1.70×10^{-7}	1.90×10^{-7}	553 032	848 430
- 1.10	1 325 052		2.23×10^{-7}		910 796	
- 1.25		1 946 244		6.86×10^{-7}		
- 1.30	1 747 073	2 982 229	8.02×10^{-7}	8.75×10^{-7}		
- 1.35	2 820 465	3 532 432	9.36×10^{-7}	1.04×10^{-6}		

Table 2 Electron binding energy from Figs. 5(a) and 5(b)

Nickel	$\Phi_{\text{Ni}^0 2p_{3/2}}$ / eV	$\Phi_{\text{Ni}^0 2p_{1/2}}$ / eV	$\Phi_{\text{Ni}_2\text{O}_3 2p_{3/2}}$ / eV	$\Phi_{2p_{3/2}-2p_{1/2}}$ / eV
Standard ^[18]	852.30	869.70	855.60	17.40
Nickel coating	851.83	869.14	855.58	17.30
$n\text{-Al}_2\text{O}_3/\text{Ni}$ coating	851.89	868.80	855.80	17.60

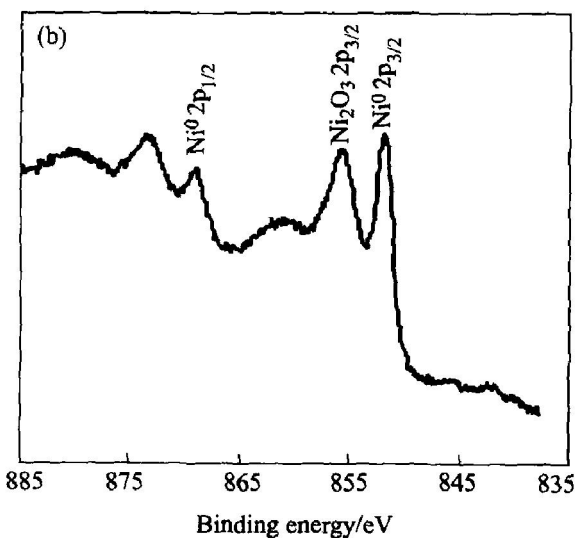
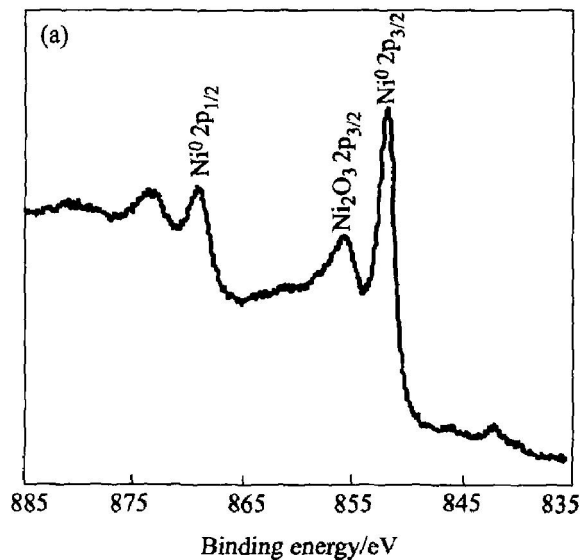


Fig. 5 XPS spectra of nickel

(a) —Ni coating; (b) —Al₂O₃/Ni composite coating

Fig. 6 shows the XPS spectrograms of aluminium from the nano-alumina powder and alumina in the composite coating.

The binding energy of Al2p in composite coating is 0.7 eV lower than that in the powder. This is a piece of very important evidence about the chemical combination between nanoparticle and matrix metal. The result proves that there is chemical bond between nano-alumina and nickel and aluminium atoms are inclined to acquire electron.

In composite coating, the main component contain nickel, oxygen and aluminium, the electronegativity of oxygen and nickel are higher than that of aluminium, it is impossible that aluminium directly captures electron from oxygen or nickel, the binding energy of Al2p does not seem to be decreased. The experimental result can be explained reasonably as follows: the unsaturated chemical bond of oxygen on nano-alumina surface can combine with nickel adatom and leads to the increasing

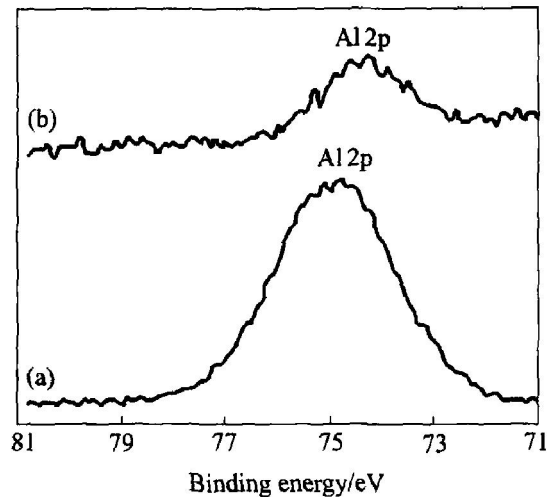


Fig. 6 XPS spectra of aluminum

(a) —Al₂O₃ powder;

(b) —Al₂O₃/Ni composite coating

of the electron cloud density outside of oxygen atom nucleus, and part of the electron cloud can be transferred to outside of aluminium atom nucleus near this oxygen atom. So the electron cloud density outside of aluminium atom nucleus increases while binding energy decreases.

The information gotten by XPS reveals the chemical state of the interface between matrix metal and nanoparticles in composite coating. The above facts demonstrates that there is chemical bond between nano-alumina and matrix nickel.

3.5 Co-deposition mechanism of nano-alumina

The main processes of metal electrodeposition include reactant transfer in liquid, interface reaction and electrocrystallization on electrode surface. Al₂O₃ has no electrochemical activity itself and no electron exchange will happen between nanoparticle and electrode. Therefore nanoparticles has no effect on the electron exchange reaction and its effect will be at the subsequent crystallization process.

The nanoparticles have enormous surface, the crystal field and binding energy of atoms on surface are different from those of interior atoms. There are many crystal defects and unsaturated chemical bonds on the nanoparticles surface^[20, 21], the unsaturated oxygen atom can combine with nickel adatom strongly. During the electrodeposition process, nano-alumina and Ni²⁺ are firstly carried to the neighbourhood of the electrode by brush plating pen, then they arrive at the electrode surface through fluid boundary layer. Ni²⁺ is reduced and becomes adatom on electrode surface, simultaneously some of nano-alumina are captured by electrode surface. Some of the captured nanoparticles combining weakly with electrode are carried away from the electrode surface by friction of brush pen

and convection of solution, while the nanoparticles combining strongly with electrode surface are held on the growing surface of metal. During the electrocrystallization, the absorbed nickel atoms would diffuse on the electrode surface. Some of diffusing adatoms can arrive at the interface between captured nanoparticles and growing metal surface and combine with unsaturated chemical bond of oxygen atom on the surface of nano-alumina. As a result, Ni—O chemical bond forms and these nickel atoms become the new nucleation and growing sites. Nanoparticles are embedded gradually in the newly deposited nickel atoms, which leads to the formation of the composite coating.

On the surface of nanoparticles, the probable combining position for Ni atoms should be the defect location, where the unsaturated chemical bond gathers and is easy to combine with other atoms because of its high reaction activity. Little active energy is needed for nucleation and growing. Therefore, the adatoms are easily inserted into crystal lattices and the electrodeposition rate of nickel rises. The increasing of nucleation and growth centers leads to the increasing of the number of crystal grains. The distribution coefficient of charge on each crystal grain became small, so the size of crystal decreased^[8, 10].

In general, the crystal lattice defect and dislocation on the growth metal surface is considered to be reaction activation sites, which are the probable combining sites for nanoparticles. In the brush plating process, the imperfect location on metal growing surface formed continuously, which decides the distribution of nanoparticles in composite coating. The growth, formation and performance of composite coating are closely relative to the latter.

Nanoparticles combine with matrix nickel by means of chemical bond. So the structure of composite coating is continuous. This is structure foundation on which composite coating has excellent performance.

According to experimental results, the co-deposition mechanism of nano-alumina could be summarized as follows. 1) Ni^{2+} and $n\text{-Al}_2\text{O}_3$ in solution are carried to fluid boundary layer near electrode surface by hydromechanical effect from convection of solution. 2) Ni^{2+} and $n\text{-Al}_2\text{O}_3$ arrive at electrode surface by electric field and hydromechanical effect. 3) Ni^{2+} is absorbed on the growth metal surface, acquires electrons and becomes adatom. 4) The adatom diffuses on the growth metal surface, moves to the crystal growth site and enters the metal crystal lattice. In the meantime, the adatom gathers and forms nucleus. 5) Some of the nanoparticles arriving at electrode surface are captured effectively by electrode. 6)

Some of absorbed nickel atoms diffusing on metal growing surface arrive at the interface between nanoparticles and electrode surface, react with unsaturated chemical bond of oxygen atoms on nanoparticles surface and forms Ni—O chemical bond. Some of interfaces between electrode and nanoparticles surface become new growth and nucleation centers. 7) Nanoparticles are embedded gradually in newly deposited nickel atoms. When the embedding process proceeds to some degree, nanoparticles would be inlaid in the growing metal layer forever and so the composite coating forms.

4 CONCLUSIONS

1) Nuclei density, nucleation rate constant and crystal growth rate rise with the increasing of step potentials. Nano-alumina consolidates the effect.

2) Nanoparticles are favorable for producing more growing and nucleation centers and promote the nickel electrocrystallization.

3) The unsaturated bond of oxygen on nanoparticle surface can combine with the absorbed nickel atoms by way of chemical bond. Some of interfaces between nanoparticles and metal growing surface become the new nucleation and growth sites of nickel atom.

Acknowledgments

The authors gratefully acknowledge Professor SHAO Yuan-hua and Dr. ZHAN Dong-ping of Chemistry Department of Peking University. Thanks will also be given to Professor LIU Fen, Professor ZHAO Liang-zhong and Dr. QIU Li-mei of Chemistry Institute of CAS for their experimental assistance and beneficial discussion. The particular thanks should also be extended to Professor WU Bing-liang and Professor CHEN Yong-yan of Electrochemistry Research Institute of Wuhan University for theoretic contribution.

REFERENCES

- [1] Vanek D. An update on brush plating [J]. *Metal Finishing*, 2002, 7: 18 - 20.
- [2] Dini J W. Brush plating: recent property data [J]. *Metal Finishing*, 1997, 6: 88 - 93.
- [3] Yang R P, Cai X, Chen Q L. Mechanism of hydrogen desorption during palladium brush plating [J]. *Surface and Coating Technology*, 2001, 141: 283 - 285.
- [4] Subramanian B, Sanjeeviraja C, Jayachandran M. Brush plating of tin(II) selenide thin films [J]. *Journal of Crystal Growth*, 2002, 234: 421 - 426.
- [5] Hu S B, Tu J P, Mei Z, et al. Adhesion strength and high temperature wear behavior of ion plating TiN composite coating with electric brush plating Ni/W interlayer [J]. *Surface and Coatings Technology*, 2001, 141: 174 - 181.

- [6] Clarke R D. DALIC selective brush plating and anodizing [J]. International Journal of Adhesion & Adhesives, 1999, 19: 205 - 207.
- [7] MA Ya-jun, ZHU Zhang-xiao. Progress of brush plating technology [J]. Surface Technology, 2001, 30 (6): 5 - 7.
- [8] JIANG Bin, XU Bir-shi, DONG Shi-yun, et al. Study on microstructure and contact fatigue performance of α -Al₂O₃/Ni composite coatings prepared by electrobrush plating [J]. Tribology (supplement), 2002, 22 (4): 185 - 188.
- [9] WANG Wei, GAU He-tong, GAO Jian-ping, et al. Interfacial orbital interaction in Ni/ZrO₂ composite plating and hydrogen evolution reaction [J]. Chinese Journal of Materials Research, 1997, 11(2): 143 - 147. (in Chinese)
- [10] TU Wei-yi, XU Bir-shi, JIANG Bin, et al. Study on microstructure and Co-deposition mechanism of α -Al₂O₃/Ni composite coating prepared by electrobrush plating [J]. Journal of Materials Engineering, 2003, 7: 31 - 35.
- [11] Abyaneh M Y, Fleischmann M. The electrocrystallization of nickel part II —comparison of models with the experimental data [J]. J Electroanal Chem, 1981, 119: 197 - 208.
- [12] Amblard J, Froment M, Maurin G, et al. The electrocrystallization of nickel on vitreous carbon: a kinetic and structural study of nucleation and coalescence [J]. J Electroanal Chem, 1982, 134: 345 - 352.
- [13] Amblard J, Froment M, Maurin G, et al. Nickel electrocrystallization —from nucleation to textures [J]. Electrochimica Acta, 1983, 28(7): 909 - 915.
- [14] Fletcher S. Some new formulae applicable to electrochemical nucleation/growth/collision [J]. Electrochimica Acta, 1983, 28(7): 917 - 923.
- [15] Scharifker B, Hills G. Theoretical and experimental studies of multiple nucleation [J]. Electrochim Acta, 1983, 28(7): 879 - 889.
- [16] Abyaneh M Y, Fleischmann M. The electrocrystallization of nickel (I) —generalised of models of electrocrystallization [J]. J Electroanal Chem, 1981, 119: 187 - 195.
- [17] Fleischmann M, Thirsk H R. Advances in Pure and Applied Electrochemistry (Vol. 3) [M]. New York: Interscience, 1963. 1 - 15.
- [18] Galtayries A, Grimblot J. Formation and electronic properties of oxide and sulphide films of Co, Ni and Mo studied by XPS [J]. Journal of Electron Spectroscopy and Related Phenomena, 1999, 98 - 99: 267 - 275.
- [19] Wanger C D, Riggs W M, Davis L E, et al. Handbook of X-ray Photoelectron Spectroscopy [M]. Minnesota: Perkin-Elmer Corporation Physical Electronic Division, 1979.
- [20] WU Gao-hui, YU Zhi-qiang, SUN Dong-li, et al. Rare-earth modification of sub-micron Al₂O₃ particle surface and its effect on the aging behavior of 6061Al composite [J]. The Chinese Journal of Nonferrous Metal, 2003, 39(8): 870 - 874. (in Chinese)
- [21] ZHANG Zhi-kun, CUI Zuolin. Nanometer Technology and Nanometer Material [M]. Beijing: National Defence Industry Press, 2000. (in Chinese)

(Edited by LONG Hua-zhong)